JPET Fast Forward. Published on December 18, 2007 as DOI: 10.1124/jpet.107.133975

DOXYCYCLINE ATTENUATES ISOPROTERENOL- AND TRANSVERSE AORTIC BANDING- INDUCED CARDIAC HYPERTROPHY IN MICE

Mounir Errami, Cristi L. Galindo, Amina T. Tassa, John M. DiMaio, Joseph A. Hill, and Harold R. Garner

Department of Human Growth and Development (ME, CLG, HRG), Department of Infectious Diseases (ATT), Department of Cardio-Thoracic surgery (JMD), Department of Internal Medicine (JAH) of the University of Texas Southwestern Medical Center, 2201 Inwood Road, Dallas, Texas 75390-9185

Running Title:

Doxycycline attenuates cardiac hypertrophy

Correspondence to Mounir Errami, Division of Translational Research, University of Texas Southwestern Medical Center, 2201 Inwood Road, Dallas, Texas 75390-9185, +1-214-648-5992. Fax:+1-214-648-1445 ; e-mail**:** mounir.errami@utsouthwestern.edu

Number of text pages: 32

Number of tables: 2

Number of figures: 5

Number of references: 40

Number of words in:

Abstract	250
Introduction	609
Discussion	1367

Section: Cardiovascular

List of non-standard abbreviations:

TAB/Transverse aortic banding; ACE/angiotensin converting enzyme; MMP/Matrix metalloproteases ; RT-PCR /Reverse transcriptase-polymerase chain reaction

JPET Fast Forward. Published on December 18, 2007 as DOI: 10.1124/jpet.107.133975
This article has not been copyedited and formatted. The final version may differ from this version.

Abstract

The FDA-approved antibiotic doxycycline (DOX) inhibits matrix metalloproteases, which contribute to the development of cardiac hypertrophy (CH). We hypothesized that DOX might serve as a treatment for CH. The efficacy of DOX was tested in two mouse models of CH: induced by the beta-adrenergic agonist isoproterenol (ISO) and induced by transverse aortic banding (TAB). DOX significantly attenuated CH in these models, causing a profound reduction of the hypertrophic phenotype and a lower heart-to-body weight ratio ($p<0.05$, $n \geq 6$). As expected, ISO increased MMP2 and 9 activities, and administration of DOX reversed this effect. Transcriptional profiles of normal, ISO-, and ISO+DOX-treated mice were examined using microarrays and the results confirmed by real-time RT-PCR. 206 genes were differentially expressed between normal and ISO mice that were reversibly altered between ISO- and ISO+DOX-treated mice, indicating their potential role in CH development and DOX-induced improvement. These genes included those involved in the regulation of cell proliferation and fate, stress and immune responses, cytoskeleton and extracellular matrix organization, and cardiac-specific signal transduction. The overall gene expression profile suggested that MMP2/9 inactivation was not the only mechanism whereby DOX exerts its beneficial effects. Western blot analysis identified potential signaling events associated with CH, including up-regulation of EDG1 receptor and activation of ERK, p-38, and the transcription factor ATF-2, which were reduced after administration of DOX. These results suggest that DOX might be evaluated as a potential CH therapeutic and also provide potential signaling mechanisms to investigate in the context of CH phenotype development and regression.

Introduction

Cardiac Hypertrophy (CH), in its physiological form, occurs during development and as an adaptation to exercise (i.e., the “athletic heart”) and is characterized by preserved contractile function and improved heart performance (Raskoff *et al.*, 1976). Pathological CH occurs as a consequence of biomechanical stress, such as prolonged arterial pressure overload, or valvular heart disease. This form of CH is maladaptive, because heart enlargement, though it abrogates the initial stimuli, is characterized by contractile dysfunction and a decrease in heart performance. Prolonged pathological hypertrophy is associated with a significant increase in the risk for progression to heart failure, ischemic heart disease and sudden death (Kannel *et al.*, 1969). This maladaptive process is presumably not beneficial due to the unfavorable prognosis associated with the disease and favorable outcome correlated with a reduction in mass of the left ventricle, irrespective of which type of treatment is applied (Mathew *et al.*, 2001). Prognosis for patients diagnosed with cardiac hypertrophy is typically poor, and aside from drug therapies, the only “cure” at present is a heart transplant. Despite the availability of generally acceptable therapies, such as angiotensin converting enzyme (ACE) inhibitors and beta blockers, CH remains a chronic and progressive process. More specific therapies are needed to prevent heart deterioration in individuals with hypertrophy and to reduce unwanted side effects associated with current medications.

It is not known whether a reduction in heart mass is responsible for the beneficial effects of current medications or whether it is a consequence of treatment, but it is accepted as a standard metric to assess the effect of therapies. The process of CH is complex and involves multiple cross-regulated signaling pathways (for review see Frey and Olson, 2003) that culminate in massive alterations in myocardial architecture (Fard *et al.*, 2000). Matrix metalloproteases (MMPs) are pivotal to this process as central mediators of cardiac remodeling in response to injury and/or cardiac wall stress. MMPs are abnormally

increased in a wide variety of diseases, including CH (Wainwright, 2004), and their inhibition has been demonstrated as a potential therapeutic strategy for CH (Asakura *et al.,* 2002; Chancey *et al.*, 2002; Miura *et al.*, 2003).

In this study, we used IRIDESCENT, a computational program that can detect previously unknown relationships between medical terms (e.g., small molecules, phenotypes, and genes) in Medline (Wren *et al.*, 2004), to predict potential drug therapies for CH. The utility of IRIDESCENT as a drug discovery tool was previously confirmed by predicting and verifying the relationship between chlorpromazine and CH (Wren *et al.*, 2004). In addition to several other candidates, doxycycline (DOX) was predicted as a potential therapy for pathological CH. The software identified DOX as a potential therapeutic partly because it was previously shown to generally inhibit MMPs (Griffin *et al.*, 2005), which suggested to us that it might reduce a hypertrophic phenotype. DOX is a very well-tolerated antibiotic and is also FDA approved, making it a particularly attractive candidate for CH therapy. Furthermore, DOX has been shown in ischemic-reperfusion studies to exert a protective effect, when administered prior to the induction of myocardial infarction (MI) (Griffin *et al.,* 2005; Villarreal *et al.*, 2003). In order to evaluate the efficacy of DOX, mice were treated with the drug after induction of CH with the β-adrenergic agonist, isoproterenol (ISO), or TAB. We found that DOX indeed inhibited CH-associated MMP2/9 activation and attenuated ISO- and TAB- induced CH. The potential signaling mechanisms involved were investigated by analyzing the expression and activity of various molecules that could contribute to the development of cardiac hypertrophy. A putative signaling pathway was constructed based on these results and it indicated that DOX perturbs ISO-induced up-regulation of EDG1 receptor expression and activation of ERK, p38, and ATF-2.

Methods

Animals

All animal studies were conducted in accordance with the standards set forth in the *Guide for the Care and Use of Laboratory Animals (NIH Publication No. 85-23, revised 1996)* and were approved by UT Southwestern Institutional Animal Care and Use Committee Guidelines. Experiments were performed using 3 mice per group for microarrays, 6 mice per group for aortic banding, and 10 mice per group for all others unless otherwise stated. Normal, untreated mice and mice that did not receive surgery (isoproterenol or aortic banding) but that did receive doxyclycline served as negative controls.

ISO-induced CH

Eight-week-old male C57BL/6 mice (Jackson Laboratory) were challenged with ISO (Sigma Aldrich, MO) at 40mg.kg^{-1}.d^{-1}, administered s.q. via micro-osmotic pump insertion (ALZET 1007D, Braintree Scientific, MA). Animals were anesthetized with isoflurane (1.5%) and oxygen (98.5%) with an animal ventilator (Surgivet, WI). An incision (1 cm) was made on the back of each animal between the shoulder blades, and a micro-osmotic pump containing ISO dissolved in saline solution (0.9% NaCl) was inserted into the infrascapular subcutaneous tissue. Mice were sacrificed after 7 days of experimentation.

TAB-induced CH

Increased pressure in the proximal aorta was induced by means of TAB, as previously described (Hill *et al.*, 2000). Male mice (C57Bl6, 8 weeks old) were anesthetized with ketamine (100 mg/kg IP) plus xylazine (5 mg/kg IP), orally intubated with 20-gauge tubing, and ventilated (Harvard Apparatus Rodent Ventilator, model 687) at 120 breaths

per minute (0.1-mL tidal volume). A 3-mm left-sided thoracotomy was performed at the second intercostal space. The transverse aortic arch was ligated (7-0 Prolene) between the innominate and left common carotid arteries with an overlying 27-gauge needle, and then the needle was removed, leaving a discrete region of stenosis. The chest was closed, and the left-sided pneumothorax was evacuated. Perioperative (24 hours) and 1-week mortalities were <10% each. Mice were sacrificed after 21 days of experimentation.

Administration of DOX

DOX (6mg.mL^{-1}) (Sigma Aldrich) was given in drinking water containing 5% sucrose, beginning immediately after surgery and through the remainder of the experiment. The solution was changed twice weekly because of the short half-life of DOX in water. Control animals were given 5% sucrose water without the drug.

Microarray Sample Preparation and Analysis

Animal hearts were rapidly removed and flushed with saline to remove residual blood. Total RNA was isolated from the left ventricles using TRIzol Reagent (Life Technologies, MD), per the manufacturer's instructions, purified by phenol-chloroform extraction and ethanol precipitation, and 20 μg reserved for microarray analysis. Samples were further processed, labeled, and hybridized to GeneChip Mouse Genome 430 2.0 arrays (Affymetrix) by the University of Texas Southwestern Medical Center Microarray Core. Data were analyzed using GeneSifter (VizX Labs, WA), SAM (Stanford, CA), and Spotfire DecisionSite 8.2 (Spotfire, Inc., MA).

One mouse heart was used for each array, and the experiment was performed in triplicate, generating a total of 9 arrays. GeneSifter was used to perform RMA normalization, pairwise comparisons of averaged signal intensity values, and Student's t-

test with Benjamini and Hochberg correction. Spotfire was used to perform pairwise comparisons of the individual experiments, and two-class, unpaired comparisons were made using SAM. A gene was considered as significantly altered in expression if the average fold-change value was at least 2.0, the fold-change for each individual replicate comparison was at least 1.5, the corrected p-value was less than 0.05, and the false discovery rate was less than 5%. Additionally, genes that were altered between any two WT or control samples were removed, as these alterations most likely represented normal variations among mice.

Histology

Mouse hearts were excised, fixed in 10% phosphate-buffered formalin for 48h, and then embedded in paraffin. Cross-sectional slices along the minor axis were obtained with a microtome and then stained using Mayer's Hematoxylin and Eosin (H&E) or Masson's Trichrome.

Real-time reverse transcriptase-polymerase chain reaction (RT-PCR)

Quantitative RT-PCR was performed in the iCycler iQ (Bio-Rad, CA) using SYBR Green I dye (Qiagen, CA), as described by the manufacturer. Each 25-µl reaction contained 100 ng RNA, 2.5µl of primers (Quantitect Primer Assays, Qiagen), 12.5µl SYBR Green PCR master mix, and 0.25µl reverse transcriptase. A typical protocol included reverse transcription at 50°C for 30min and a denaturation step at 95°C for 15 min followed by 35 cycles with 94°C denaturation for 15s, 55°C annealing for 30s, and 72°C extension for 30s. Detection of the fluorescent product was performed at the end of the extension period at 60°C for 20s. To confirm amplification specificity, the PCR products were subjected to a melting curve analysis. Negative controls containing water instead of RNA were concomitantly run to confirm that the samples were not cross-contaminated.

Targets were normalized to reactions performed using Quantitect GAPDH primers (Qiagen), and fold-change was determined using the comparative threshold method (Livak and Schmittgen, 2001).

MMP activity

General MMP activity was measured using the Enzolyte 520 Generic MMP assay kit (AnaSpec, CA). Briefly, hearts were homogenized in 0.15M NaCl, 20mM ZnCl, 1.5mM NaN_3, and 0.01% Triton X-100. Samples were subsequently diluted in assay buffer to equal concentration (~45µg), incubated with the FAM/QXL 520 FRET substrate at 37^{o}C for 1h in a 96-well plate, and the plate read at 490nm. APMA (4-aminophenylmercuric acetate)-treated samples served as positive controls. Zymographies were performed using Ready-Gel zymogram gels (Bio-Rad) per the manufacturer's instructions. Briefly, protein samples were diluted (1:2) in Bio-Rad zymogram sample buffer and resolved on 10% gelatin zymography gels at 100 V for 1.5 h. Sample proteases were then renatured in Bio-Rad renaturing solution for 30 min at room temperature, followed by overnight incubation in development solution at 37 ^{o}C. Gels were then stained with 0.5% Coomassie Blue R-250 for 1 h and de-stained with 40% methanol and 10% acetic acid before visualizing. Clear bands represented activated proteases, the sizes of which were compared to a positive control (MMP-2/MMP-9 zymography standard, Chemicon, Temecula, CA). MMP-2/MMP-9 Inhibitor IV (Chemicon) was used as a negative control.

Immunoblotting

Left ventricles were homogenized in 100mM Tris-HCl (pH 7.4) containing 15% glycerol, 2mM EDTA, 2% SDS, and 0.1mM phenylmethylsulfonylfluoride. Homogenates were heated at 95°C for 10 min, passed through a 23-gauge needle five times, and centrifuged at 12,000g for 10min (Chen *et al.*, 2001). Proteins (80µg/ml) were resolved

by 10% SDS-PAGE and electrophoretically transferred onto a nitrocellulose membrane (Amersham Hybond, GE Healthcare, NJ). Membranes were blocked with 5% milk (Bio-Rad, CA) and probed with affinity-purified antibodies at 1:1000 dilution. Membranes were subsequently incubated with horseradish peroxidase-conjugated secondary antibody (Cell Signaling Technology, MA) and then exposed to chemiluminescence substrate (GE Healthcare). Affinity-purified anti-MMP2, anti-EDG-1, and anti-GAPDH antibodies were purchased from Santa Cruz, and anti-phospho-p-38, anti-total p-38, anti-phospho-ERK, anti-total ERK, and anti-phospho-ATF-2 antibodies were obtained from Cell Signaling Technology.

Statistical Analysis

Values presented are expressed in mean ± standard error of the mean (SEM). All comparisons between groups were performed using a one tail Student's t-test. Differences were considered statistically significant for $p<0.05$.

Results

Attenuation of CH as measured by heart-to-body weight ratios

DOX significantly attenuated ISO- and TAB- induced heart-to-body ratios, which is a marker for cardiac hypertrophy, in mice (heart-to-body weight ratios were 6.0±.3 mg/g for ISO treated mice versus 5.0±.1 mg/g for ISO+DOX treated mice, $p<0.05$; n=11 per group; Figure 1). The reduction of the CH phenotype in the hearts of mice that received DOX, compared to control mice that received ISO treatment alone, was clearly visible in heart cross sections (Figure 1-C). Further, DOX attenuation of the hypertrophic phenotype was comparable to Captopril, an ACE inhibitor that is commonly prescribed by physicians to patients with hypertension, heart failure and CH. DOX-induced reduction in heart size was more pronounced on the left side. Heart-to-body weight ratios and histological appearance of hearts for mice that received DOX but not ISO were comparable to untreated mice (data not shown). Essentially the same results were obtained when TAB was used to induce hypertrophy, rather than ISO treatment (heart-to-body weight ratios were 5.8±.2 mg/g for TAB treated mice versus 5.3±.1 mg/g for TAB mice treated with DOX, p-value<0.05, n = 6 per group; data nor shown).

MMP activity

General MMP activity was measured in the hearts of normal mice and those treated with ISO or ISO plus DOX. As shown in Figure 2A, ISO induced general MMP activity, compared to untreated mice. This level of general MMP activity did not further increase after treatment with APMA, a known activator of MMPs and positive control. General MMP activity was abrogated when mice were treated with DOX and ISO, with activity levels similar to those of control mice. These data were reproducible and statistically significant. We also examined the protein level of MMP2, the activation of which is strongly correlated with adverse myocardial remodeling and increased heart size (Soini

et al., 2001). As shown in Figure 3, there was no appreciable increase in MMP2 protein levels in CH mice, with or without drug treatment. Similarly, MMP9 was not increased at the level of transcription, based on real-time RT-PCR results (data not shown). Zymographies indicated that the activity levels of both MMP2 (Figure 2B) and MMP9 (Figure 2C) were increased after ISO treatment and reduced with DOX administration. Based on microarray results and real-time RT-PCR (Tables 1 and 2), MMP3 was up-regulated in mice with ISO-induced CH (7.4-fold) and down-regulated after DOX treatment (2.9-fold). MMP3, which was previously shown to be substantially increased in dilated cardiomyopathy (Spinale *et al.*, 2000), can degrade a wide range of extracellular proteins, as well as activate other MMPs. While no other MMPs were found to be transcriptionally altered, based on microarray results (Supplemental Table 1) and Western blot analysis of MMP2 (Figure 3), an increase in general MMP activity in CH mice that was abrogated by DOX treatment was confirmed (Figure 2).

Effect DOX on Gene Expression Profile

To assess the effect of DOX on cardiac gene expression, microarray analysis was performed on normal mice (WT) and mice with ISO-induced CH that were subsequently untreated (control) or treated with DOX. Based on the microarray analysis criteria (see methods), there were 354 genes that were altered in expression between control and DOX treated mice, 206 of which (Supplemental Table 1) were specific to the disease (i.e., also altered between WT and control mice, but in the opposite direction as that observed for control versus DOX treated mice). In other words, genes that were up-regulated by ISO treatment (compared to WT mice) were down-regulated by DOX treatment (compared to control mice), and genes that were down-regulated by ISO treatment were up-regulated by DOX treatment. These 206 genes included those involved in the regulation of cell proliferation and fate, stress and immune responses,

cytoskeletal and extracellular matrix organization, and cardiac-specific signal transduction. Eighteen of these genes were selected for verification by real-time RT-PCR (Table 1). Examples of genes previously reported to be associated with cardiac hypertrophy, which were up-regulated in mice with ISO-induced CH and down-regulated after DOX treatment are shown in Table 2.

Endothelial differentiation sphingolipid G-protein-coupled receptor 1 (EDG1) was up-regulated (2.5-fold) in CH mice and down-regulated (2.4-fold) subsequent to DOX treatment (Table 2), which was confirmed at the protein level and Western blot analysis (Figure 4). Likewise, TBRII is up-regulated (2.4-fold) in mice with ISO-induced CH and returned to normal after DOX treatment (Table 2). CDKN1A was also profoundly up-regulated (14.6-fold) in mice with ISO-induced CH and subsequently down-regulated (6.5-fold) by DOX. CDKN1A, MAP3k6 and Map3k8, which are activators of the c-Jun N-terminal kinase (JNK) pathway, were both up-regulated (5.90-fold and 2.68-fold, respectively) in CH mice, based on microarray analysis results (Table 2). Conversely, the major ventricular gap junction protein, connexin 43, was down-regulated (3.89-fold) in CH mice and returned to normal levels (up-regulated 3.61-fold) in response to DOX treatment.

Finally, among the interesting observations, Adenosine deaminase (ADA) was up-regulated (2.14-fold) in CH mice and returned to baseline levels (down-regulated 2.41-fold) in response to DOX treatment (Table 2). The activity of ADA, an enzyme involved in nucleotide metabolism and immune responses has been shown to be increased in cardiac hypertrophy induced by aortocaval shunt, coarctation of the abdominal aorta or by thyrotoxicosis (Czarnowski *et al.*, 1996).

Post-translational Effects of DOX Administration

In addition to examination of DOX-induced transcriptional changes, we also investigated several proteins known to be associated with hypertrophy-related signaling pathways, as detailed in the literature. As shown in Figure 4, the phosphorylated version of the mitogen-activated protein kinase (MAPK) ERK 1/2 and stress-associated p-38 MAPK were up-regulated in mice with CH and reduced subsequent to DOX treatment. Alteration of these proteins was specific for the activated forms, as antibodies that recognize both the phosphorylated and non-phosphorylated versions (total ERK and total p-38) did not result in bands that differed substantially in size or intensity between conditions (Figure 4). Phosphorylation of the down-stream MAPK transcription factor ATF-2 was similarly increased in ISO mice and depressed after DOX treatment (Figure 4). We also examined the protein levels of an upstream receptor, EDG-1, which based on microarray results, was transcriptionally up-regulated in ISO mice and returned nearly to baseline after DOX treatment. Western blot analysis confirmed this trend, as shown in Figure 4. Anti-GAPDH antibodies served as an internal control to ensure equal protein was loaded on the gels (Figure 4).

Discussion

MMPs are known to contribute to the development of various heart defects, including CH and MI, and DOX, an FDA-approved drug with a known absorption/toxicity profile, has been shown to inhibit MMPs (Golub *et al.,* 1998; Grenier *et al.*, 2002; Griffin *et al.*, 2005). This prompted us to test the drug in two different mouse models of CH. This study demonstrates the efficacy of DOX in attenuating CH in both ISO-induced and TAB associated CH. Hypertrophy in animals that did not receive DOX treatment was characterized by an increase in heart wall thickness, especially on the left side, which was expected, given the increased workload of the left ventricle. This paper reports for the first time that an FDA-approved antibiotic is effective in reducing the cardiac hypertrophy phenotype.

Human oral DOX therapy currently involves a dosage of approximately 3mg/kg/day, given over a period of time ranging from 1 week to 60 days. The dosage used in this study (6mg/mL in drinking water) is as much as 15 to 20 times higher than the human allometric equivalent (assuming mice drink approximately 3mL/day on average). We chose this higher dosage in order to ensure that the effects observed would be reproducible and because we did not observe a statistically significant reduction in heart size when the human equivalent dose was used in preliminary experiments. Also, this treatment regimen (6mg/mL in drinking water) had been previously used in another study, which investigated the efficacy of DOX for the treatment of muscular dystrophy in mice (Davies *et al.*, 2006). However, we did test the ability of 4mg/mL treatments to reduce CH (data not presented), which recapitulated the effects of the higher dosage (6mg/mL). Additional dose ranging experiments are required to firmly establish the minimal effective dose of DOX and to confirm its therapeutic potential to regress pre-established CH. Also, a less acute form of hypertrophy, such as a spontaneous hypertensive rat model, which is more representative of slowly progressive heart

disease, might better demonstrate potential beneficial effects of DOX at lower dosages. A different method of DOX administration might further improve the resolution of these experiments, as delivery in water does not allow for precise control of dosage. Apart from its ability to inhibit MMP2/9, the underlying mechanism of DOX-induced attenuation of CH is not clear. The majority of genes that were altered in response to ISO treatment and returned to baseline levels after DOX administration were not obviously related to MMP expression or activity. This indicated to us that other signaling mechanisms might contribute to the beneficial effects of DOX.

Figure 5 details the proposed signaling events that occur in ISO mice that are perturbed by DOX treatment, based on microarray and Western blot analyses and on previously reported research. As shown, ISO could lead to TGFβ pathway signaling via TBRII up-regulation. When bound by its ligand (TGFβ), the TBRI subunit is recruited, binds to TBRII, and then recruits the adaptor molecule, SMAD. This is known to lead to subsequent activation of p38 and SP1 transcription factor. The TGFβ pathway, when activated, has also been shown to cause activation of TAK1, which activates JNK. Our results indicate that ISO might cause JNK activation via an alternate route, engagement of the EDG1 receptor by its ligand sphingosine 1 phosphate (S1P), as shown Figure 5. Stimulation of the EDG1 receptor, which was up-regulated in CH mice and down-regulated subsequent to DOX treatment (Table 2) induces cardiac hypertrophy (Robert *et al.*, 2001). The precise molecular events that occur between S1P-engagement of EDG1 and cardiac hypertrophy are not known, but S1P has been shown to induce phosphorylation of stress-activated JNK protein kinase *in vitro* (Robert *et al.*, 2001), which might be activated in response to ISO and reversed by DOX treatment, based on the results of this study. Yet another potential mechanism for JNK activation is phosphorylation of upstream MAPKs (Map3k6/Map3k8), each of which were shown to

be up-regulated transcriptionally based on microarray results (Table 2). JNK activation leads to down-regulation of connexin 43 and activation of ATF-2 transcription factor, which causes up-regulation of MMPs, such as MMP2/9, and CDKN1A. The pathways shown have been associated with cardiac remodeling, based on multiple literature reports. DOX could perturb these signaling events by preventing up-regulation of TBRII and EDG1 (Figure 5).

JNK, which is a major player in the process of cardiac hypertrophy and myocardial extracellular matrix remodeling, is activated under a variety of pathological conditions, including hypertension, ischemia/reperfusion injury, and myocardial infarction (Li *et al.,* 1998; Pellieux *et al.*, 2000). Upstream (Map3k6 and Map3k8) and downstream (ATF-2) signaling events detected in our study (Table 2 and Figure 4) indicate that JNK is likely activated by ISO and inhibited by DOX. Initially, the activation of JNK in response to cardiac stress could be protective (Tachibana *et al.*, 2006), but extended activation most likely leads to hypertrophy. For example, JNK activation contributes to remodeling of gap junctions that leads to loss of ventricular wall compliance and a profound decrease in epicardial conduction velocity (Petrich and Wang, 2004; Petrich *et al.*, 2004) and was previously shown to cause reduction in connexin 43 levels (Petrich *et al.*, 2004). Loss of connexin 43 has been shown to lead to ventricular dysfunction and cardiac arrhythmia, a lethal eventuality of progressive heart failure (Gutstein *et al.*, 2001). Further, patients with de-compensated cardiac hypertrophy have been shown to have diminished levels of connexin 43, compared to patients with compensated hypertrophy, and connexin 43 has thus been proposed to significantly contribute to a maladaptive response to cardiac stress and subsequent heart failure (Kostin *et al.*, 2004). However, we were unable to obtain evidence that JNK is produced in normal mice or in response to ISO or DOX treatment, by Western blot analysis. This could have been due to technical difficulties, or perhaps the JNK pathway is bypassed in our system. We are currently designing

experiments to address this issue in order to delineate the role of JNK, if any in ISO-induced CH and reversal of the CH phenotype by DOX.

Transforming growth factor-β (TGF-β) activity has also been linked to cardiac hypertrophy. For instance, TGF-β has been shown to mediate a hypertrophic response in cardiomyocytes in response to angiotensin II (Ikeuchi *et al.,* 2004; Rosenkranz, 2004). TGF-β signaling involves binding to TGF-β receptor II (TBRII), which results in recruitment of TBRI and subsequent phosphorylation of SMAD proteins (Yu *et al.*, 2002). TBRII has also been recently shown to link TGF-β signaling and MAPK pathways via activation of TGF-β activated protein kinase 1 (TAK1) (Watkins *et al.,* 2006; Yu *et al.*, 2002), which occurs in response to pressure overload generated by aortic constriction and leads to cardiac hypertrophy and heart failure (Zhang *et al.*, 2000). Down-regulation of the expression of TBRII in response to DOX treatment would thus presumably inhibit TGF-β-induced hypertrophy. Likewise, CDKN1A, which is up-regulated via SP1 and SMAD activation subsequent to TGF-β engagement of its receptor (Chuang *et al.*, 2007), might contribute to ISO-induced hypertrophy, because it is believed to be associated with cardiac pathophysiology and pressure overload (Ohki *et al.*, 2004). Further, DOX has been previously shown to down-regulate TGF-β signaling that leads to downstream activation of SMADs and MAPKs (ERK, p38, and JNK) and subsequent stimulation of MMPs (Kim *et al.,* 2005; Li *et al.*, 2004). ERK in particular is associated with increased cardiac cell growth in response to mechanical stress (Abeles *et al.*, 2006), and like JNK, p38 has been shown to phsophorylate ATF-2, which contributes to cardiac hypertrophy (Fischer *et al.*, 2001). Considered together, this study corroborates previous research and suggests additional signaling molecules that could be involved in CH and that are inhibited by DOX administration. An overview of these hypothesized signaling events is shown in Figure 5.

In summary, we have demonstrated that the FDA-approved antibiotic, DOX, is effective in attenuating CH in mice and could therefore be investigated as a potential treatment for CH in humans. DOX is a generic drug, and testing would be relatively rapid and inexpensive compared to non-FDA-approved drug candidates. Dose studies could determine if DOX is indeed suitable for human CH trials, and administration in mice suggests that it could additionally serve as a cardiovascular research tool.

Acknowledgments

The authors wish to thank L. Danielle Olson for excellent technical aid and Linda Gunn for administrative assistance.

References

Abeles D, Kwei S, Stavrakis G, Zhang Y, Wang ET and Garcia-Cardena G (2006) Gene expression changes evoked in a venous segment exposed to arterial flow. *J Vasc Surg*. **44**:863-870.

Asakura M, Kitakaze M, Takashima S, Liao Y, Ishikura F, Yoshinaka T, Ohmoto H, Node K, Yoshino K, Ishiguro H, Asanuma H, Sanada S, Matsumura Y, Takeda H, Beppu S, Tada M, Hori M and Higashiyama S (2002) Cardiac hypertrophy is inhibited by antagonism of ADAM12 processing of HB-EGF: metalloproteinase inhibitors as a new therapy. *Nat Med*. **8**:35-40.

Chancey AL, Brower GL, Peterson JT and Janicki JS (2002) Effects of matrix metalloproteinase inhibition on ventricular remodeling due to volume overload. *Circulation*. **105**:1983-1988.

Chen Z, Chua CC, Ho YS, Hamdy RC and Chua BH (2001) Overexpression of Bcl-2 attenuates apoptosis and protects against myocardial I/R injury in transgenic mice. *Am J Physiol Heart Circ Physiol*. **280**:H2313-2320.

Chuang T, Guh J, Chiou S, Chen H, Hung W and Chuang L (2007) Sp1 and Smad3 are required for high glucose-induced p21(WAF1) gene transcription in LLC-PK(1) cells. *J Cell Biochem*. In press.

Czarnowski D, Wojcik B, Langfort J and Gorski J (1996) 5'-Nucleotidase and adenosine deaminase activities in hypertrophied rat heart. The effect of tachycardia. *Rocz Akad Med Bialymst*. **41**:334-340.

Davies JE, Berger Z and Rubinsztein DC (2006) Oculopharyngeal muscular dystrophy: potential therapies for an aggregate-associated disorder. *Int J Biochem Cell Biol*. **38**:1457-1462.

Fard A, Wang CY, Takuma S, Skopicki HA, Pinsky DJ, Di Tullio MR and Homma S (2000) Noninvasive assessment and necropsy validation of changes in left ventricular mass in ascending aortic banded mice. *J Am Soc Echocardiogr*. **13**:582-587.

Fischer TA, Ludwig S, Flory E, Gambaryan S, Singh K, Finn P, Pfeffer MA, Kelly RA and Pfeffer JM (2001) Activation of cardiac c-Jun NH(2)-terminal kinases and p38-mitogen-activated protein kinases with abrupt changes in hemodynamic load. *Hypertension*. **37**:1222-1228.

Frey N and Olson EN (2003) Cardiac hypertrophy: the good, the bad, and the ugly. *Annu Rev Physiol*. **65**:45-79.

Golub LM, Lee HM, Ryan ME, Giannobile WV, Payne J and Sorsa T (1998) Tetracyclines inhibit connective tissue breakdown by multiple non-antimicrobial mechanisms. *Adv Dent Res*. **12**:12-26.

Grenier D, Plamondon P, Sorsa T, Lee HM, McNamara T, Ramamurthy NS, Golub LM, Teronen O and Mayrand D (2002) Inhibition of proteolytic, serpinolytic, and progelatinase-b activation activities of periodontopathogens by doxycycline and the non-antimicrobial chemically modified tetracycline derivatives. *J Periodontol*. **73**:79-85.

Griffin MO, Jinno M, Miles LA and Villarreal FJ (2005) Reduction of myocardial infarct size by doxycycline: a role for plasmin inhibition. *Mol Cell Biochem*. **270**:1-11.

Gutstein DE, Morley GE and Fishman GI (2001) Conditional gene targeting of connexin43: exploring the consequences of gap junction remodeling in the heart. *Cell Commun Adhes*. **8**:345-348.

Hill JA, Karimi M, Kutschke W, Davisson RL, Zimmerman K, Wang Z, Kerber RE and Weiss RM (2000) Cardiac hypertrophy is not a required compensatory response to short-term pressure overload. *Circulation*. **101**:2863-2869.

Ikeuchi M, Tsutsui H, Shiomi T, Matsusaka H, Matsushima S, Wen J, Kubota T and Takeshita A (2004) Inhibition of TGF-beta signaling exacerbates early cardiac dysfunction but prevents late remodeling after infarction. *Cardiovasc Res*. **64**:526-535.

Kannel WB, Gordon T and Offutt D (1969) Left ventricular hypertrophy by electrocardiogram. Prevalence, incidence, and mortality in the Framingham study. *Ann Intern Med*. **71**:89-105.

Kim H, Luo L, Pflugfelder SC and Li D (2005) Doxycycline inhibits TGF-beta1-induced MMP-9 via Smad and MAPK pathways in human corneal epithelial cells. *Invest Ophthalmol Vis Sci*. **46**:840-848.

Kostin S, Dammer S, Hein S, Klovekorn WP, Bauer EP and Schaper J (2004) Connexin 43 expression and distribution in compensated and decompensated cardiac hypertrophy in patients with aortic stenosis. *Cardiovasc Res*. **62**:426-436.

Li D, Chen Z, Song XJ, Luo L and Pflugfelder SC (2004) Stimulation of matrix metalloproteinases by hyperosmolarity via a JNK pathway in human corneal epithelial cells. *Invest Ophthalmol Vis Sci*. **45**:4302-4311.

Li WG, Zaheer A, Coppey L and Oskarsson HJ (1998) Activation of JNK in the remote myocardium after large myocardial infarction in rats. *Biochem Biophys Res Commun*. **246**:816-820.

Livak KJ and Schmittgen TD (2001) Analysis of relative gene expression data using real-time quantitative PCR and the 2(-Delta Delta C(T)) Method. *Methods*. **25**:402-408.

Mathew J, Sleight P, Lonn E, Johnstone D, Pogue J, Yi Q, Bosch J, Sussex B, Probstfield J and Yusuf S (2001) Reduction of cardiovascular risk by regression of electrocardiographic markers of left ventricular hypertrophy by the angiotensin-converting enzyme inhibitor ramipril. *Circulation*. **104**:1615-1621.

Miura S, Ohno I, Suzuki J, Suzuki K, Okada S, Okuyama A, Nawata J, Ikeda J and Shirato K (2003) Inhibition of matrix metalloproteinases prevents cardiac hypertrophy induced by beta-adrenergic stimulation in rats. *J Cardiovasc Pharmacol*. **42**:174-181.

Ohki R, Yamamoto K, Ueno S, Mano H, Misawa Y, Fuse K, Ikeda U and Shimada K (2004) Transcriptional profile of genes induced in human atrial myocardium with pressure overload. *Int J Cardiol*. **96**:381-387.

Pellieux C, Sauthier T, Aubert JF, Brunner HR and Pedrazzini T (2000) Angiotensin II-induced cardiac hypertrophy is associated with different mitogen-activated protein kinase activation in normotensive and hypertensive mice. *J Hypertens*. **18**:1307-1317.

Petrich BG and Wang Y (2004) Stress-activated MAP kinases in cardiac remodeling and heart failure; new insights from transgenic studies. *Trends Cardiovasc Med*. **14**:50-55.

Petrich BG, Eloff BC, Lerner DL, Kovacs A, Saffitz JE, Rosenbaum DS and Wang Y (2004) Targeted activation of c-Jun N-terminal kinase in vivo induces restrictive cardiomyopathy and conduction defects. *J Biol Chem*. **279**:15330-15338.

Raskoff WJ, Goldman S and Cohn K (1976) The "athletic heart". Prevalence and physiological significance of left ventricular enlargement in distance runners. *JAMA*. **236**:158-162.

Robert P, Tsui P, Laville MP, Livi GP, Sarau HM, Bril A and Berrebi-Bertrand I (2001) EDG1 receptor stimulation leads to cardiac hypertrophy in rat neonatal myocytes. *J Mol Cell Cardiol*. **33**:1589-1606.

Rosenkranz S (2004) TGF-beta1 and angiotensin networking in cardiac remodeling. *Cardiovasc Res*. **63**:423-432.

Soini Y, Satta J, Maatta M and Autio-Harmainen H (2001) Expression of MMP2, MMP9, MT1-MMP, TIMP1, and TIMP2 mRNA in valvular lesions of the heart. *J Pathol*. **194**:225-231.

Spinale FG, Coker ML, Bond BR and Zellner JL (2000) Myocardial matrix degradation and metalloproteinase activation in the failing heart: a potential therapeutic target. *Cardiovasc Res*. **46**:225-238.

Tachibana H, Perrino C, Takaoka H, Davis RJ, Naga Prasad SV and Rockman HA (2006) JNK1 is required to preserve cardiac function in the early response to pressure overload. *Biochem Biophys Res Commun*. **343**:1060-1066.

Villarreal FJ, Griffin M, Omens J, Dillmann W, Nguyen J and Covell J (2003) Early short-term treatment with doxycycline modulates postinfarction left ventricular remodeling. *Circulation*. **108**:1487-1492.

Wainwright CL (2004) Matrix metalloproteinases, oxidative stress and the acute response to acute myocardial ischaemia and reperfusion. *Curr Opin Pharmacol*. **4**:132-138.

Watkins SJ, Jonker L and Arthur HM (2006) A direct interaction between TGFbeta activated kinase 1 and the TGFbeta type II receptor: implications for TGFbeta signalling and cardiac hypertrophy. *Cardiovasc Res*. **69**:432-439.

Wren JD, Bekeredjian R, Stewart JA, Shohet RV and Garner HR (2004) Knowledge discovery by automated identification and ranking of implicit relationships. *Bioinformatics*. **20**:389-398.

Yu L, Hebert MC and Zhang YE (2002) TGF-beta receptor-activated p38 MAP kinase mediates Smad-independent TGF-beta responses. *EMBO J*. **21**:3749-3759.

Zhang D, Gaussin V, Taffet GE, Belaguli NS, Yamada M, Schwartz RJ, Michael LH, Overbeek PA and Schneider MD (2000) TAK1 is activated in the myocardium after pressure overload and is sufficient to provoke heart failure in transgenic mice. *Nat Med*. **6**:556-563.

Footnotes

The authors also wish to thank the Hudson Foundation and the P.O'B. Montgomery Distinguished Chair for supporting this project. Additional support was provided by UT Southwestern Cardiology Fellowship, NHLBI HL007360 (CLG).

Legend for Figures

Figure 1:Top- *DOX effect on ISO-induced CH.* Each point represents one mouse. All mice were C57BL/6J, 8 weeks males. ISO was given at 40mg/kg/day s.q. (osmotic pumps). Squares represent ISO treated mice (n=11); circles represent ISO+DOX treated mice, DOX was given at 5mg/mL in 5% sucrose drinking water, beginning immediately after surgery and through the remainder of the experiment (n=11); stars represent mice treated with Captopril (drug prescribed in blood pressure overload); triangles represent normal untreated mice (n=11). Student's t-test DOX vs. Control p-value is highly significant ($p<0.001$). Letters (A,B,C) represent hearts, pictured below the graph. Similar results were obtained using heart-weight-to-tibia length ratios. Bottom- *Representative Histological cross section of hearts of Normal, ISO- and ISO+DOX treated mice.* A) Normal mouse (C57BL/6J) Heart weight (HW) = 0.1305 g; body weight (BW) = 26.3g. B) ISO treated mouse HW=0.1730g, BW=28.7g; C) ISO+DOX treated mouse HW=0.1398, BW=26.8.

Figure 2: A) General MMP activity assays results for normal mice compared to ISO and ISO+DOX mice (6 mice per group). Values are represented as mean±S.E.M. AFU = the average fluorescence unit (490 nm), and the asterisk denotes statistical significance based on Student's t test for ISO treated compared to ISO+DOX treated mice (p value = 0.0037). No statistical difference was detected between normal and ISO+DOX treated mice. B) Zymography for MMP2 activity, with "+" representing Gelatinase (a positive control). C) Zymography showing MMP9 activity. Arrows indicate MMP2 or 9 activity. No differences were found between normal mice and mice that received vehicle (saline) + DOX (not shown).

Figure 3: MMP Western Blots. Western blots were performed using heart lysates from untreated mice (Wild Type: WT); ISO treated (1, 2) and ISO+DOX treated mice (3, 4). Lysates were subjected to immunoblot analysis of MMP2 and GAPDH (used as a quantitative control). Figure shown is representative of three individual experiments.

Figure 4: Intracellular Signaling. Western blots were performed using heart lysates from untreated mice (Wild Type: WT); ISO treated mice (1, 2) and ISO+DOX treated mice (3, 4). Lysates were subjected to immunoblot analysis of phospho-ERK 1/2, total ERK 1/2 phospho-p-38, total p-38, phospho-ATF-2, EDG1, and GAPDH (used as a quantitative control). Results shown are representative of at least three individual experiments.

Figure 5: Putative ISO-induced intracellular signaling pathways that are abrogated in response to DOX treatment, based on microarray analysis. DOX: doxycycline, TGF: Transforming growth factor-β, TBR: TGF receptor, EDG1: Endothelial differentiation sphingolipid G-protein-coupled receptor 1, JNK: c-Jun N-terminal kinase, Map3k6/8: mitogen-activated protein kinase kinase kinase 6/8, CDK1NA: Cyclin-dependent kinase inhibitor 1A (p21), ATF-2: activating transcription factor-2, FOS: FBJ osteosarcoma virus, ERK 1/2: extracellular signal regulated 1/2.

JPET Fast Forward. Published on December 18, 2007 as DOI: 10.1124/jpet.107.133975
This article has not been copyedited and formatted. The final version may differ from this version.

Table 1. Real-time RT-PCR results for selected genes

		Microarray		***Real-time RT-PCR***	
Gene name	***Function***	***WT vs ISO***	***ISO vs ISO+DOX***	***WT Vs ISO***	***ISO vs ISO+DOX***
		FC			
DNA-damage-inducible transcript 4 (Ddit4)	Hypoxic stress response; cell growth	7.4	-5.6	13.9	-5.7
Matrix metalloproteinase 3 (Mmp3)	Extracellular matrix remodeling	7.4	-2.9	5.3	-3.5
Metallothionein 1 (MT2)	NO-mediated signal transduction	15.6	-5.5	19.7	-14.9
Tubulin, alpha 4 (Tuba4)	Microtubule-based movement	-6.2	5.8	-26	36.8
Actin, alpha 2, smooth muscle, aorta (Acta2)	Cytoskeletal organization; muscle development	-3.8	3.7	-9.9	9.9
Serine protease inhibitor 2-2 (Spi2-2) (Serpin3n)	Acute-phase response; inflammation	40.5	-9.7	90.5	-3.8
Transformation related protein 53 inducible nuclear protein 1 (Trp53inp1)	Stress response; apoptosis	4.8	-3.5	6.1	-1.9
NADPH oxidase 4 (Nox4)	Electron transport; superoxide release	4.3	-3.2	22.6	-4
Gem GTPase (Gem)	Calcium channel blockage	2.7	-2.8	8	-1.8

JPET Fast Forward. Published on December 18, 2007 as DOI: 10.1124/jpet.107.133975
This article has not been copyedited and formatted. The final version may differ from this version.

Oncostatin receptor (Osmr)	Inflammation; connective tissue production; extracellular matrix turnover	5.1	-2.6	Induced*	Reduced*
Phospholipase A2 group VII (platelet-activating factor acetylhydrolase, plasma) (Pla2g7)	Inflammation; lipid catabolism	3.7	-2.2	7.5	-1.9
SET and MYND domain containing 1 (Smyd1)	Heart development	-2.9	2.7	-1.7	1.6
Lipocalin 2 (Lcn2)	Vascular remodeling; apoptosis	27.7	-13.3	64	-9.9
Cyclin-dependent kinase inhibitor 1A (p21) (Cdkn1a)	Cell cycle arrest	14.6	-6.5	128	-7
S100 calcium binding protein A8 (calgranulin A) (S100a8)	Cell proliferation; calcium signaling	7.1	-19.9	5.7	-181
S100 calcium binding protein A9 (calgranulin B) (S100a9)	Cell proliferation; calcium signaling	7.1	-14	17.2	-10.4
Angiogenin, ribonuclease A family, member 1 (Ang1)	Angiogenesis	2.5	-2.1	2.5	-1.5
Cyclin G2 (Ccng2)	Cell cycle regulation	3.4	-3.1	9.2	-5.7
Myosin, heavy polypeptide 7, cardiac muscle, beta (Myh7)	Muscle contraction	2.6	-5.4	2.3	-2.5
Cytokine inducible SH2-containing protein 3 (Socs3)	Regulation of cell growth; negative regulation of insulin signaling	8.2	-5.9	9.9	-4

*Induced/reduced are used instead of fold-changes where no transcript was detected in one of the two samples being compared.

WT = untreated mice, ISO = mice with CH induced by isoproterenol treatment, and ISO+DOX = ISO mice treated with doxycycline

JPET Fast Forward. Published on December 18, 2007 as DOI: 10.1124/jpet.107.133975
This article has not been copyedited and formatted. The final version may differ from this version.

Table 2. Examples of genes altered in response to ISO-induced CH and DOX treatment, based on microarrays

Gene ID	Gene Name	Association with CH	WT vs ISO	ISO vs ISO + DOX
NM_007746	Map3k8	Cell cycle regulation; activation of JNK	2.7	-3.0
NM_016693	Map3k6	Activation of JNK	5.9	-3.2
BG793483	TBRII	TGF-β1 receptor; activation of TAK1 and SMADs	2.4	-2.3
BB133079	EDG1	Angiogenesis and calcium overload	2.5	-2.4
M63801	CX43	Regulation of heart contraction rate; vascular remodeling	-3.9	3.6
NM_010809	MMP3	Extracellular matrix remodeling; activation of other MMPs	7.4	-2.9
NM_007398	ADA	Nucleic acid metabolism; immune response	2.1	-2.4
AK007630	CDKN1A	Cell cycle arrest	14.6	-6.5
NM_007392	α-actin	Cytoskeletal organization; muscle development	-3.8	3.7
M656153	LOX	Connective tissue modeling	7.4	-2.7
AV026617	FOS	Transcription regulation; regulation of cell proliferation and differentiation	2.5	-3.9

WT = untreated mice, ISO = mice with CH induced by isoproterenol treatment, and ISO+DOX = ISO mice treated with doxycycline

JPET Fast Forward. Published on December 18, 2007 as DOI: 10.1124/jpet.107.133975
This article has not been copyedited and formatted. The final version may differ from this version.

Figure 1

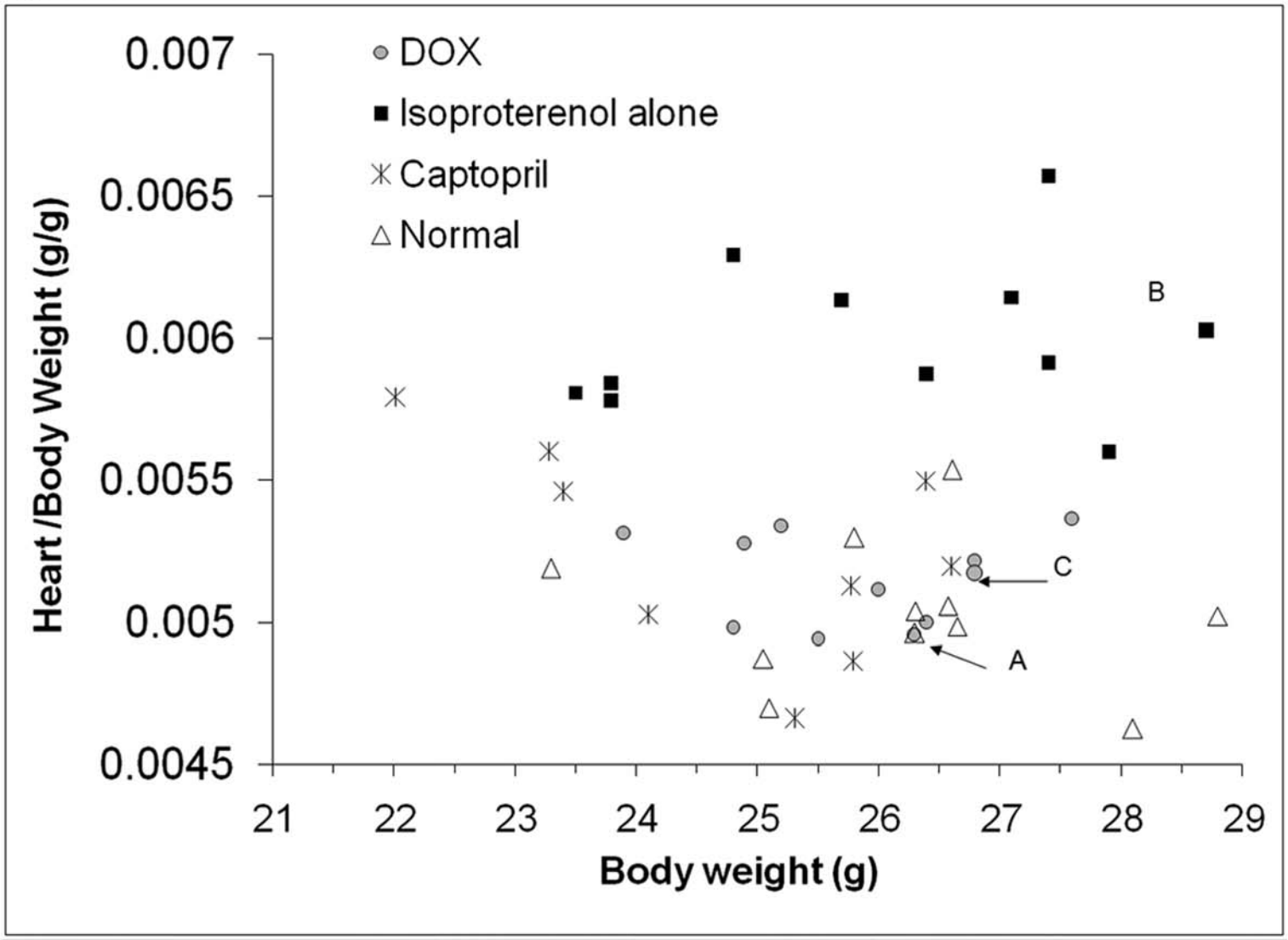

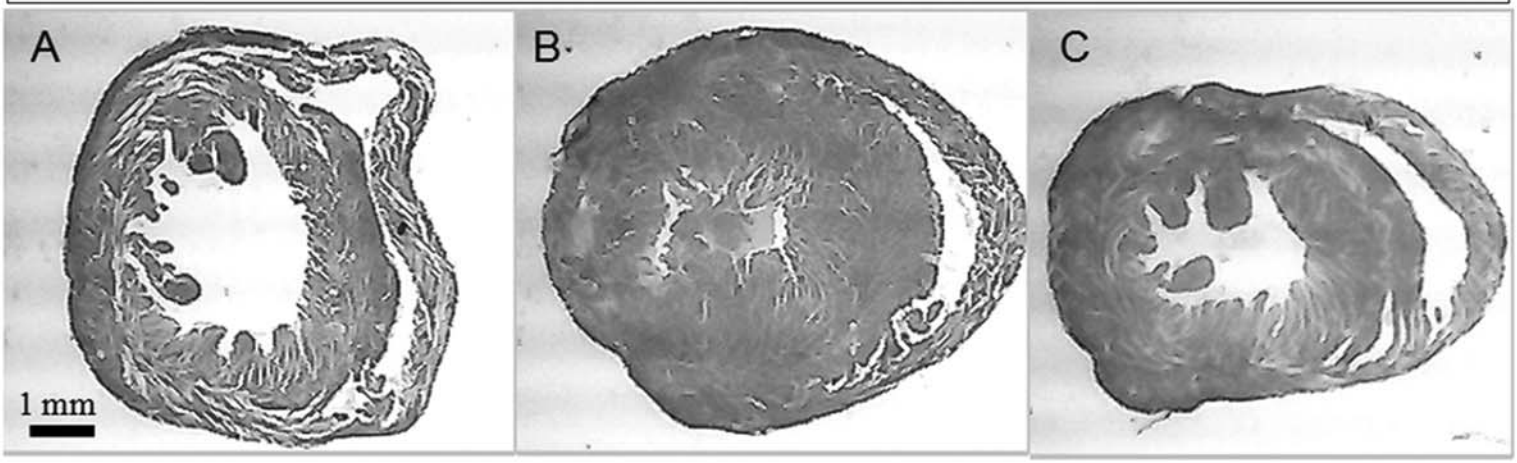

Figure 2

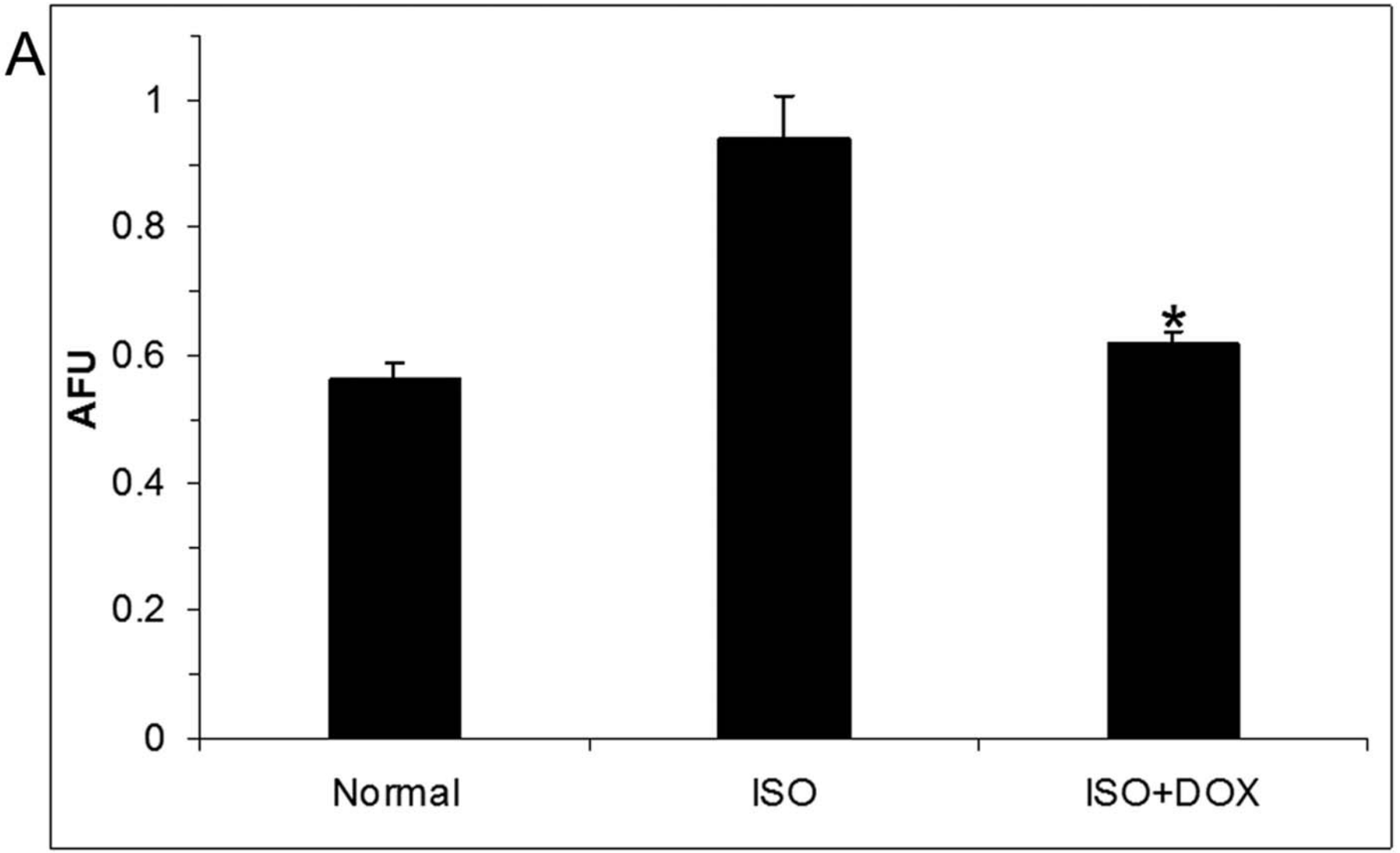

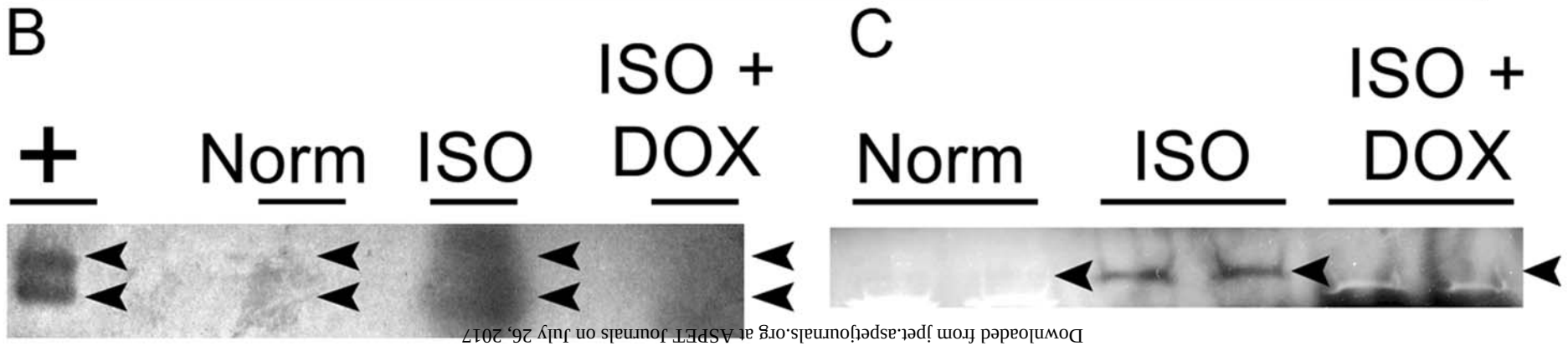

JPET Fast Forward. Published on December 18, 2007 as DOI: 10.1124/jpet.107.133975
This article has not been copyedited and formatted. The final version may differ from this version.

Figure 3

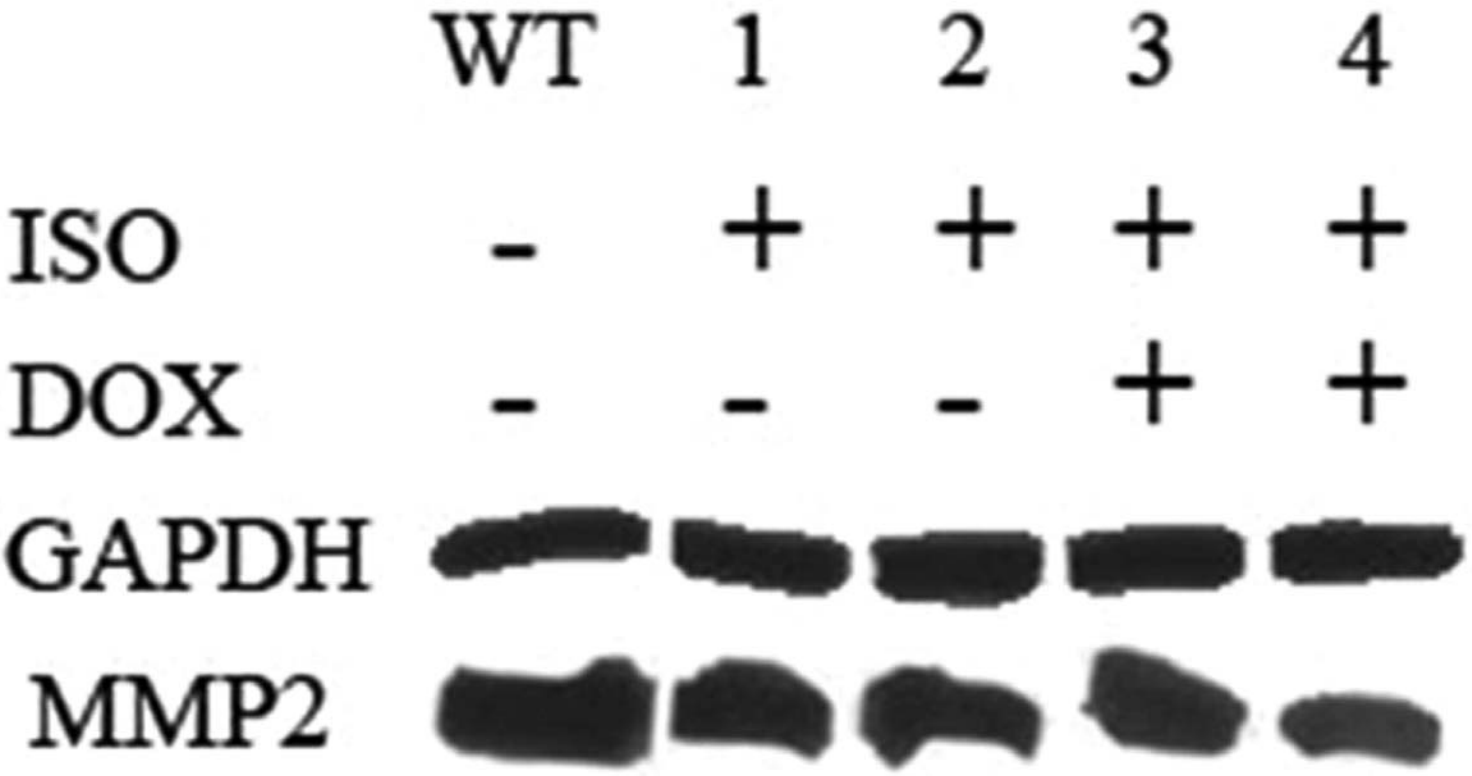

Figure 4

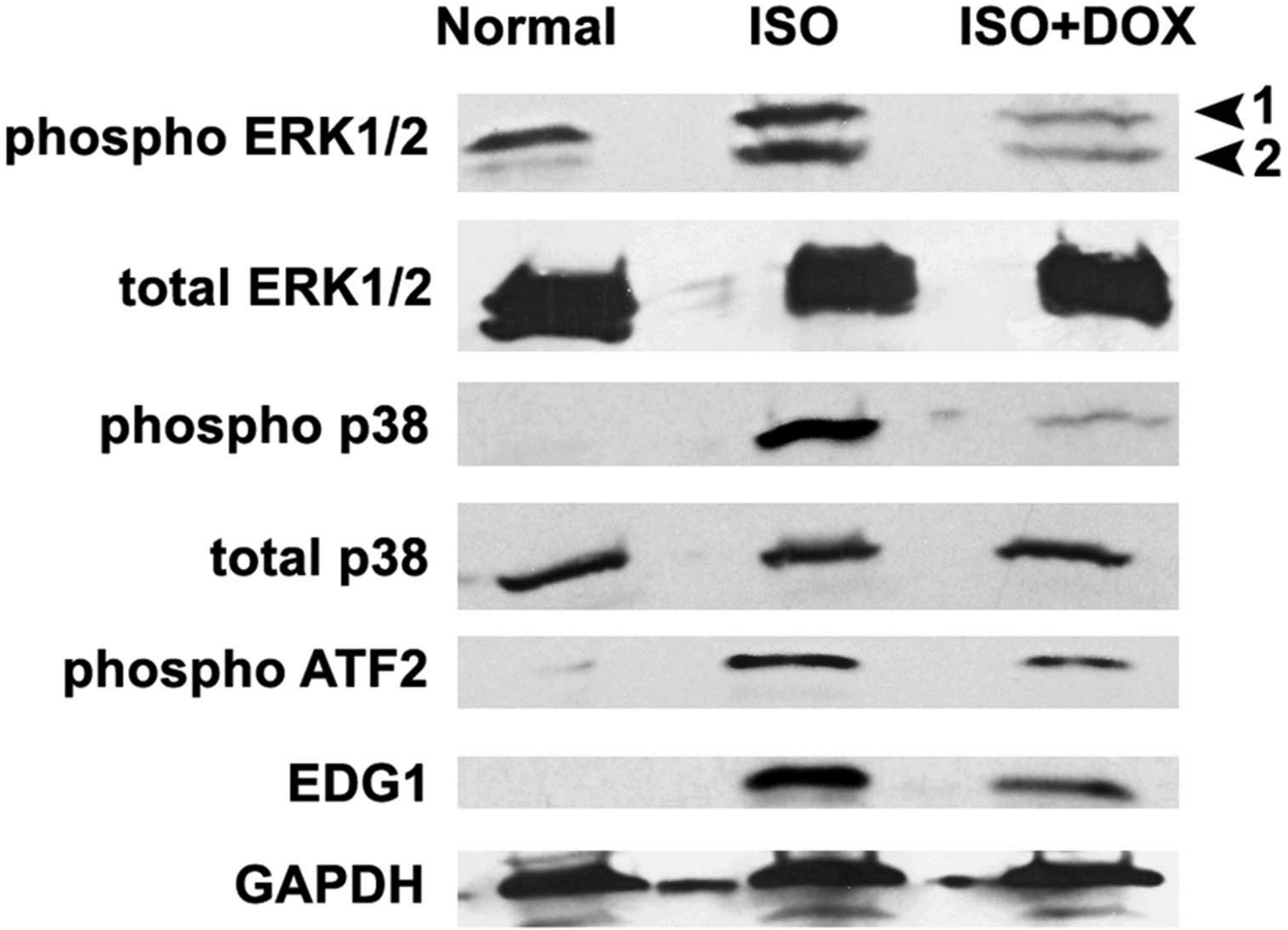

Figure 5